

International Congress of Science and Technology of Metallurgy and Materials, SAM -  
CONAMET 2013Investigation on  $\text{Al}_2\text{O}_3$ -Reinforced Zinc-Aluminum Matrix  
CompositesMarco Zurko<sup>a</sup>, Carlos Enrique Schvezov<sup>a,b</sup>, Alicia Esther Ares<sup>a,b,\*</sup><sup>a</sup>*Faculty of Sciences, University of Misiones, 1552 Félix de Azara Street, 3300 Posadas-Misiones, Argentina.*<sup>b</sup>*Member of CIC of the National Science Research Council of Argentina (CONICET).*

---

**Abstract**

Composite materials obtained by adding particles to the metallic matrix (MMCs) have made remarkable progress in its development and applications in automotive and aerospace industries in recent decades. Among them the most current application is MMCs with zinc and aluminum matrix. The present work is focused on the study of the effect of the directional heat extraction on the alumina distribution inside the zinc-aluminum matrix and on the columnar – to – equiaxed (CET) phenomenon in samples directionally solidified. The ZA-27 alloy was reinforced with ceramic-particulates of alumina ( $\text{Al}_2\text{O}_3$ ) and then vertically directionally solidified. The following parameters were measured: cooling rates, temperature gradients, interphase velocities. And the influence of heat transfer on the solidification microstructure of the MMCs was analyzed. Experimental results include transient metal/mould heat transfer coefficients, secondary dendrite arm spacings and particle distribution as a function of solidification conditions imposed by the metal/mould system. The results about the conditions for the CET in MMCs are compared with those obtained in directional solidification of Zn-Al alloys.

© 2015 The Authors. Published by Elsevier Ltd. This is an open access article under the CC BY-NC-ND license

(<http://creativecommons.org/licenses/by-nc-nd/4.0/>).

Selection and peer-review under responsibility of the scientific committee of SAM - CONAMET 2013

**Keywords:** Directional solidification, Metal matrix composites,  $\text{Al}_2\text{O}_3$ , Zn-Al.

---

---

\* Corresponding author. Tel.: +0054-376-4422186-156; fax: +0054-376-4425414.

E-mail address: [aares@fceqyn.unam.edu.ar](mailto:aares@fceqyn.unam.edu.ar)

## 1. Introduction

Composite materials are formed by combining two or more materials in such a way that the constituents are still distinguishable and not fully blended. This type of material takes advantage of the different strengths and abilities of its different elements. The majority of composite materials use two constituents: a binder or matrix and reinforcement. The reinforcement is stronger and stiffer, forming a sort of backbone, while the matrix keeps the reinforcement in a set place. The binder also protects the reinforcement, which may be brittle or breakable (Karni et al. 1994). Generally, composites have excellent compressibility combined with good tensile strength, making them versatile in a wide range of situations. Microsized ceramic powders and fibers were widely used in the fabrication of Al and Zn-based composites. Compared to the unreinforced aluminum alloy, these composites not only have a considerably improved strength and stiffness, but also a significantly reduced ductility, which limits their widespread use (Auras and Schvezov, 2004).

The columnar-to-equiaxed transition (CET) is directly associated with the existence of equiaxed grains in the melt ahead of the columnar growing front. The level of understanding of CET was summarized by Spittle 2006, whereas a comparison of different CET prediction methods was given very recently by Mc Fadden et al. 2009.. The interaction between parameters involved in the CET has obtained considerable interest over the last decades in order to understand the structure evolution of ingot castings and to optimize metallurgical processes (Hunt 1984, Ziv and Weinberg 1989, Ares and Schvezov 2000, Ares et al. 2002, Ares et al. 2005, Ares and Schvezov 2007, Gandin 2000, Gandin 2000, Reinhart et al 2005, Spittle 2006, Yasuda et al. 2006, Mc Fadden et al. 2009, Gueijman et al. 2010).

The aim of the present investigation was to analyze the effect of the directional heat extraction on the microstructure of composites and on  $\text{Al}_2\text{O}_3$  distribution in the aluminum matrix composite during the columnar – to – equiaxed (CET) position in samples directionally solidified. Zn-27wt.%Al (ZA27) alloy matrix was reinforced/filled with ceramic-particulates of alumina ( $\text{Al}_2\text{O}_3$ ), vertically directionally solidified. The following parameters were measured: cooling rates, temperature gradient and interphase velocities. And the influence of heat transfer on the solidification microstructure of the MMCs was analyzed. Experimental results include grain size and particle distribution as a function of solidification conditions imposed by the metal/mold system. The conditions for the CET in MMCs are compared with those in Zn-Al alloys.

## 2. Experimental details

The metal matrix composites were prepared from zinc (99.98 wt pct) and commercial aluminum (99.96 wt pct) and adding  $\text{Al}_2\text{O}_3$  particles. The compositions of composites are shown in Table 1. The samples were melted and solidified directionally upwards in an experimental setup described elsewhere (Ares and Schvezov 2000, Ares et al. 2002, Ares et al. 2005, Ares and Schvezov 2007). The temperature measurements were performed using K-type thermocouples which were protected with ceramic shields. The thermocouples were previously calibrated using four temperature points: demineralized water at the freezing and boiling points (corrected by atmospheric pressure) and zinc (99.98 wt pct) and aluminum (99.96 wt pct) at their melting points. The accuracy of thermocouples was determined to be between  $\pm 0.5$  K. The samples were melted in Pyrex® molds of 29 mm-E.D. and 27 mm-I.D.

The liquidus and solidus temperatures for each alloy were determined by the start and the end of solidification at each thermocouple position. Both points were detected by changes in the slopes of the cooling curve at the start and the end of solidification. This criterion was chosen in order to allow undercooling to occur before solidification and possible recalescence during solidification of equiaxed grains. The values of temperatures are shown in Table 1. The results between both methods are within 5% error and within the predicted values given by the phase diagram (Moffat 1984). After solidification, the samples were cut in an axial direction, polished with emery paper up to 1000 grit and 1- $\mu\text{m}$  alumina using a low speed machine and etched with a mix containing chromic acid (50 g  $\text{Cr}_2\text{O}_3$ , 4 g  $\text{Na}_2\text{SO}_4$  in 100 mL of water) during approximately 10 seconds at room temperature (Vander Voort 2000). The position of the transition was located by visual observation and optical microscopy and the distance from the chill zone of the sample was measured with a ruler. The average grain size and volume fraction were determined according to ASTM E 112-88 and ASTM E 562-89 techniques, respectively. The size, volume and number of particles in three dimensions were determined utilizing Saltykov's modification of Johnson's method (Underwood 1968). The determination of the number of particles by means of a grid method was done dividing one section in 64

squares of 20 X 20 mm uniformly distributed. The number of repetitions in each case ensured a representative distribution in each sample. The particle volume distribution was obtained utilizing the standard norm ASTM E562-89. The determination of the density of averages sizes of particles was found quantifying the repetitions of size of different particles in the grid utilized. An average of the distribution of sizes was obtained. The range of particles size is between 1,56  $\mu\text{m}$  to 20,79  $\mu\text{m}$  of average diameter.

The microstructure was analyzed with optical and scanning electron microscopy (SEM). The distribution of elements in the microstructure was determined using EDXA. A Rigaku X-ray diffraction (XRD) system (Rigaku MSC, the Woodlands, TX) was used for the XRD analysis of the alloys and composites.

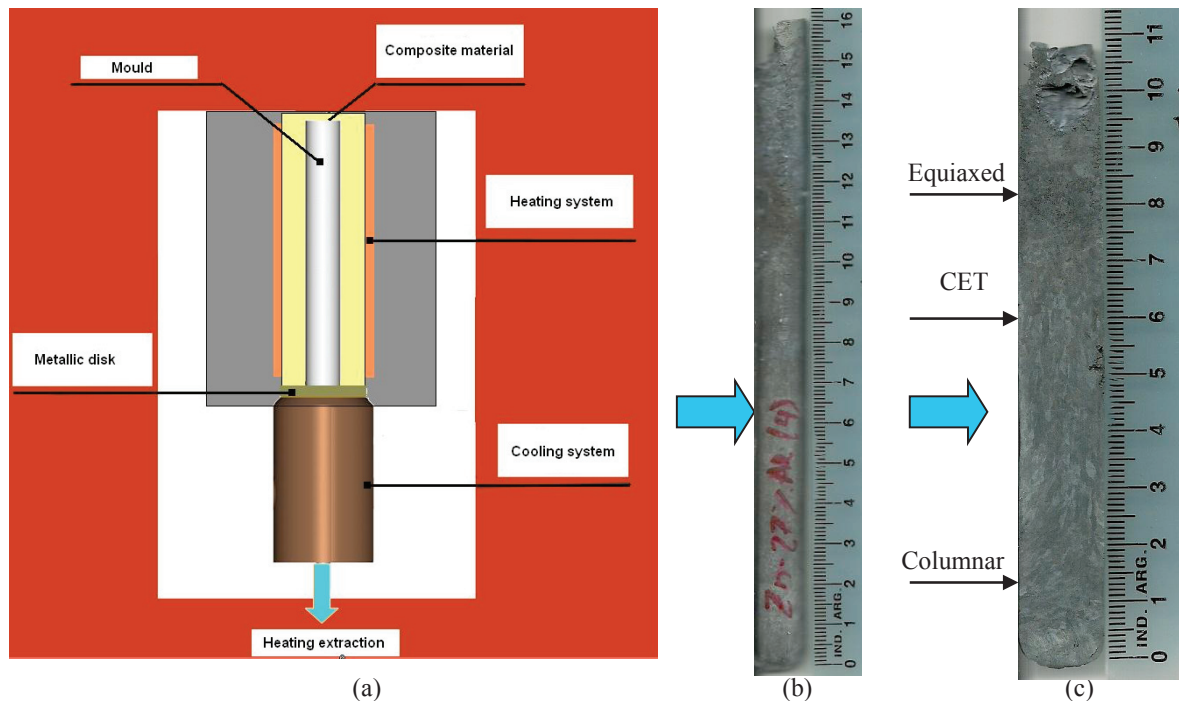


Fig. 1. (a) Experimental setup. (b) Composite sample. (c) Macrostructure showing different structures.

### 3. Results and Discussion

#### 3.1. Macrostructures and microstructures

A number of twelve experiments in a range of alloy and composite compositions and cooling rates were performed. A typical macrostructures of the transition is shown in Figure 2 for: (a) ZA27+5vol%Al<sub>2</sub>O<sub>3</sub>, (b) ZA27+8vol%Al<sub>2</sub>O<sub>3</sub> and (c) for ZA27+16vol%Al<sub>2</sub>O<sub>3</sub>. As was reported elsewhere for other alloys (Ares and Schvezov 2000, Ares et al. 2002, Ares et al. 2005, Ares and Schvezov 2007, Gueijman et al. 2010), the transition is not sharp showing a zone where some equiaxed grains co-exist with columnar grains. The size of the transition zone is in the order of up to ten millimeters between the minimum position of the CET (CET<sub>Min.</sub>) and the maximum position of the CET (CET<sub>Max.</sub>). Also, no effect of the set of the thermocouples in the transition is observed; either acting as nucleating sites or changing the solidification structure.

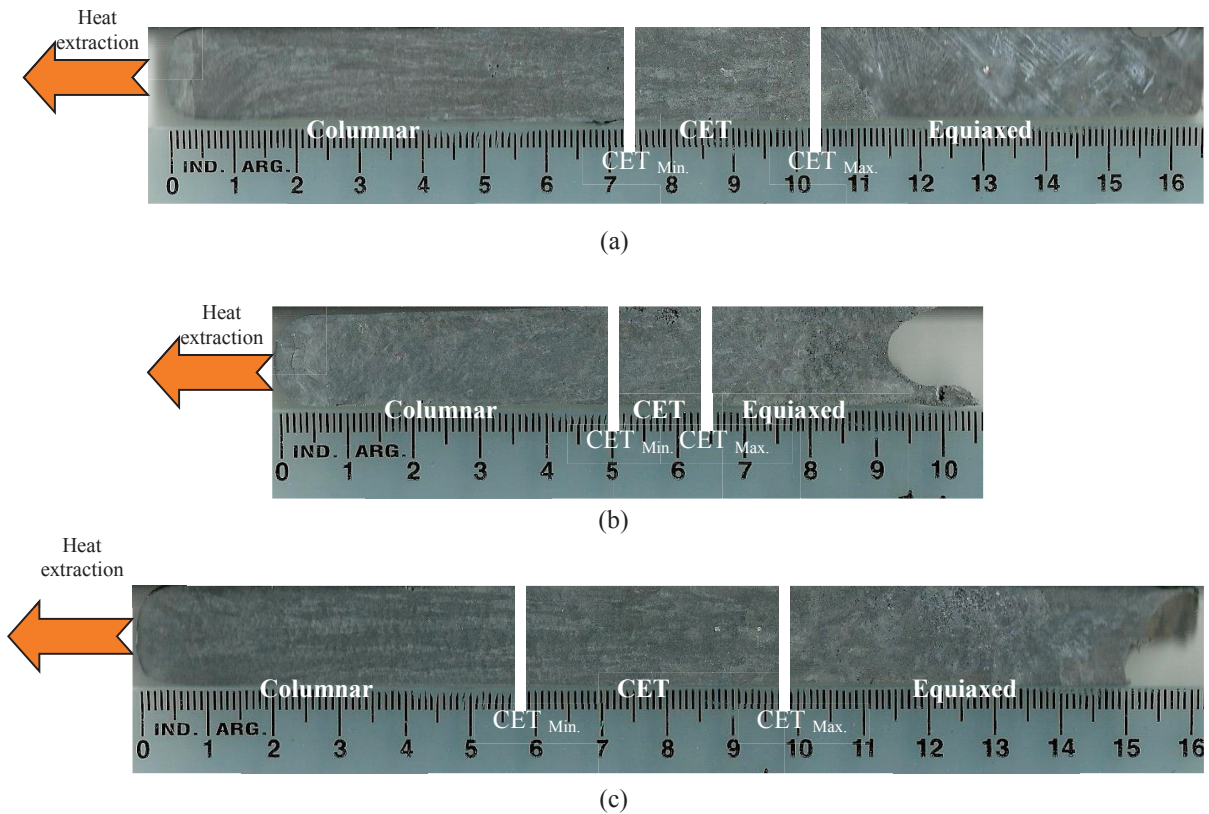


Fig. 2. Macrostructures of three different composites showing the CET. (a) ZA27+5vol%Al<sub>2</sub>O<sub>3</sub>.  
(b) ZA27+8vol%Al<sub>2</sub>O<sub>3</sub>. (c) ZA27+16vol% Al<sub>2</sub>O<sub>3</sub>.

The solidification microstructure of the ZA27 alloy (Figure 3) presents a dendritic structure consisting of  $\alpha$  primary dendrites rich in aluminum. The  $\alpha + \eta$  eutectoid is formed from  $\alpha$  dendrites and  $\beta$  peritectic through a transformation at 548 K, following the Zn-Al phase diagram and formed during the final stage of solidification. This eutectoid has a typical platelike form of  $\alpha$  and  $\eta$  sheets and a standard and a finer eutectic structure is observed.

Al<sub>2</sub>O<sub>3</sub> appears in the interdendritic zone of the microstructure. Figure 3 shows the matrix with particles of Al<sub>2</sub>O<sub>3</sub>.

Some degree of porosity is present in the samples, which increases from the bottom to the top of the casting as can be seen in Figure 4. This porosity was observed in the case of directional solidification of SiC-reinforced Zinc-Aluminum matrix composites (Ares and Schvezov 2010, Ares and Schvezov 2013).

The size of particles range is between 1,75 Pm to 15,8 Pm in average diameter. In position 3 (top of the sample) there are no particles higher than 7.02 Pm, whereas in position 2, the size distribution is more homogeneous than in other positions. In position 1 (bottom of the sample) it is possible to appreciate particles of 5.26 Pm of average diameter, that is, about twice with respect to the other positions.



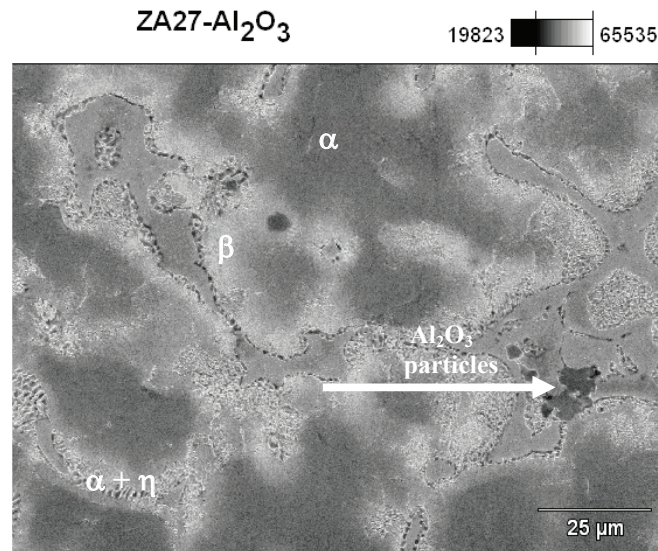


Fig. 3. Microstructures of one Zn-27wt.%Al+Al<sub>2</sub>O<sub>3</sub> alloy. The  $\alpha + \eta$  eutectoid is formed from  $\alpha$  dendrites and  $\beta$  peritectic through a transformation at 548 K, following the Zn-Al phase diagram and formed during the final stage of solidification.

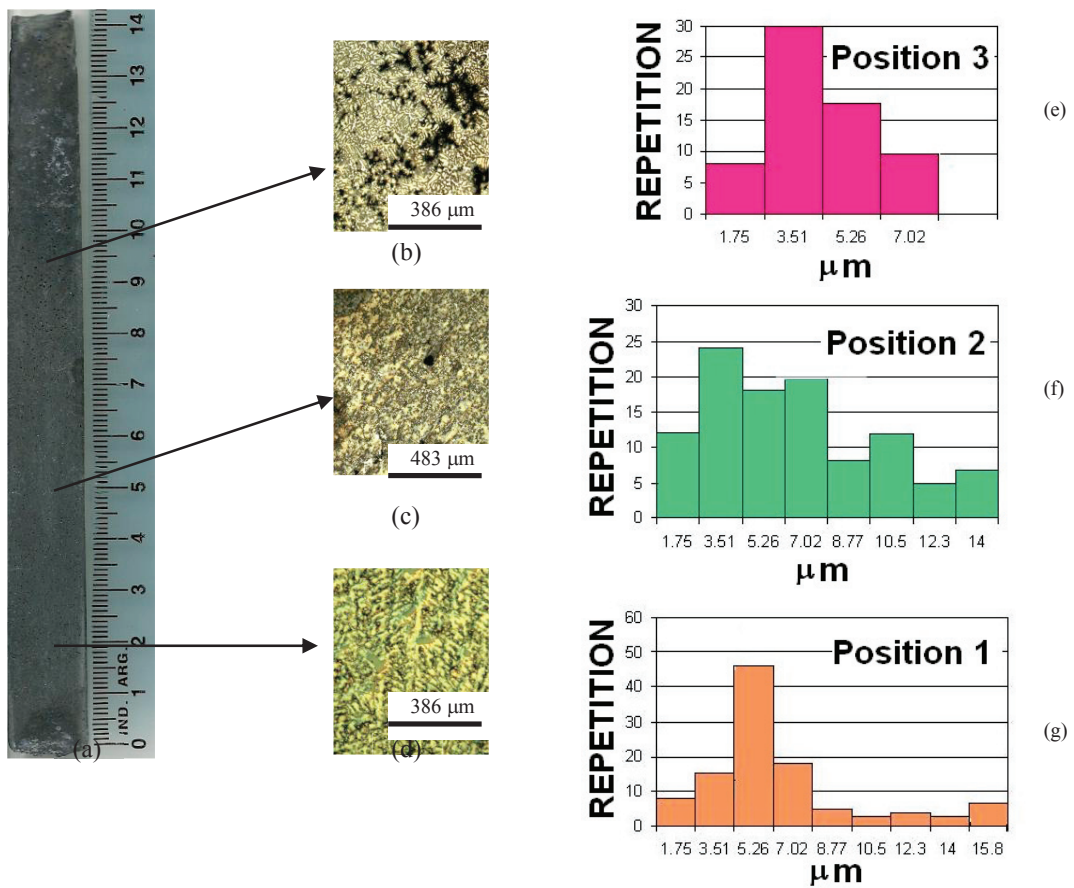


Fig. 4. Distribution of particles in function of position and size. ZA27+8vol%Al<sub>2</sub>O<sub>3</sub> sample.

### 3.2. Cooling velocity

As reported before (Ares and Schvezov 2000, Ares et al. 2002, Ares et al. 2005, Ares and Schvezov 2007, Gueijman et al. 2010) the cooling velocity of the liquid alloy was determined from the temperature versus time curves at each thermocouple position and taking the average slope. The temperature versus time plot for one experiment is presented in Figure 5 (a). The cooling velocities calculated from the type of curves in Figure 5 (b) are listed in Table 1 for all the experiments as  $\dot{T}_L$ . Table 1 also lists the location of the transition from the bottom of the sample which is in the range of  $CET_{Min.}$  to  $CET_{Max.}$  (cm). Comparing the cooling velocities with the distances which correspond to the length the columnar zone, it is observed that increasing the velocity increases the length of the columnar grains ( $CET_{Max.}$ ). As it was observed for ZA alloys in previous research (Ares and Schvezov 2007), the temperature versus time curves also show that the temperature evolution depends on the structure being formed. During columnar solidification the temperature decreases steadily and monotonically, on the contrary in the equiaxed region, during the transition, there is a recalescence which increases the temperature from a minimum; the level of recalescence for each experiment is listed in Table 1 as REC (°C).

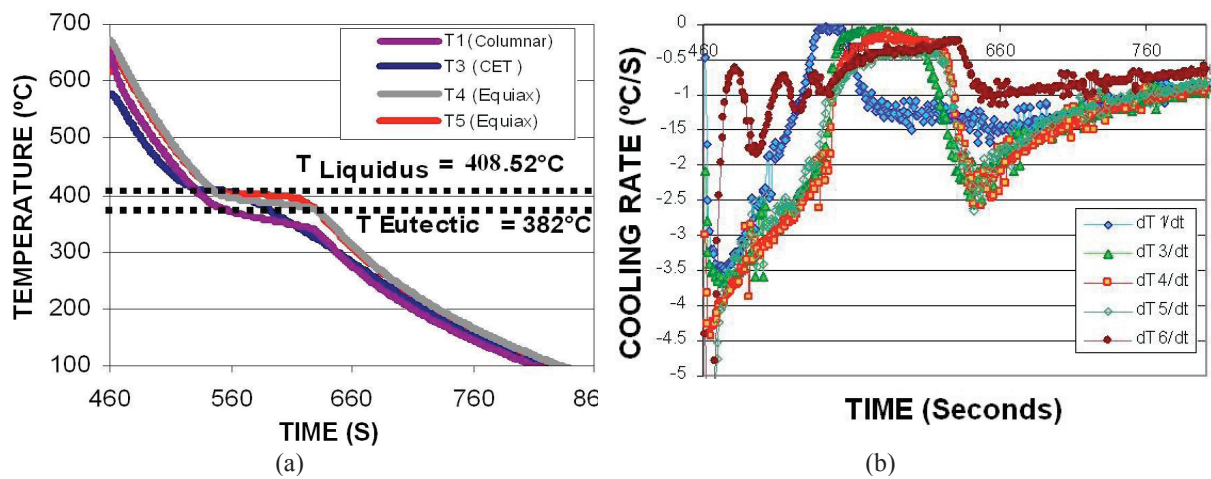


Fig. 5. Composite cooling curves. T1 is the thermocouple at the lowest position (in the base) and T5 is at the highest position (on the top).

Table 1. Cooling velocity of the liquid ( $\dot{T}_L$ ), Cooling velocity of the solid ( $\dot{T}_S$ ), Minimum CET position ( $CET_{Min.}$ ) and Maximum CET position ( $CET_{Max.}$ ), Critical gradients ( $G_C$ ) and recalescence values (REC.) obtained from the temperature versus time curves.

#	Alloy and Composite	$\dot{T}_L$ (K/s)	$\dot{T}_S$ (K/s)	$CET_{Min.}$ (mm)	$CET_{Max.}$ (mm)	$G_C$ (K/mm)	REC (°C)
1	Zn-27wt.%Al (ZA27)	3.3	1.0	35	85	-0.37	2.3
2	Zn-27wt.%Al (ZA27)	2.2	1.4	21	44	0.1	1.0
3	Zn-27wt.%Al (ZA27)	2.5	1.8	29	56	0.63	3.0
4	ZA27+5vol% $Al_2O_3$	3.0	1.0	24	46	-0.56	2.1
5	ZA27+5vol% $Al_2O_3$	3.6	2.4	41	64	-1.47	2.6
6	ZA27+5vol% $Al_2O_3$	3.9	2.6	72	102	0.52	2.2
7	ZA27+8vol% $Al_2O_3$	3.1	1.6	29	46	-0.01	2.8
8	ZA27+8vol% $Al_2O_3$	2.3	1.2	19	41	-1.3	3.3
9	ZA27+8vol% $Al_2O_3$	2.8	1.7	50	64	-1.81	2.7
10	ZA27+16vol% $Al_2O_3$	2.6	1.8	37	52	-0.12	2.4
11	ZA27+16vol% $Al_2O_3$	2.1	1.0	15	41	-1.00	2.9
12	ZA27+16vol% $Al_2O_3$	3.2	2.3	57	98	-1.5	3.2

### 3.3. Solidification velocity

The solidification velocity was determined from time recorded by the beginning to the end of solidification at each thermocouple position and considering the separation between thermocouples of 20 mm. The position of the interphases for one experiment with composite is shown in Figure 6 (a). A uniform motion of the liquidus and solidus interphases as in the case of Zn-Al alloys was observed (Ares and Schvezov 2007). The horizontal bar in each position indicates the time it takes the temperature to go from the liquidus to the solidus temperature i.e. the local solidification time versus liquidus and solidus interphase. Figure 6 (b) is a schematic of the position of interphases during solidification in the sample. From these types of figures, or from Figure 6 (c), the velocities can easily be calculated for the same experiments.

In both cases an acceleration of the interphase movement which becomes particularly relevant at the transition from columnar to equiaxed solidification can be observed. Moreover, it is observed that the liquidus interphase,  $V_L$ , accelerate faster than the solidus interphase,  $V_S$ . The numerical values of both velocities at the transition are listed in Table 2.

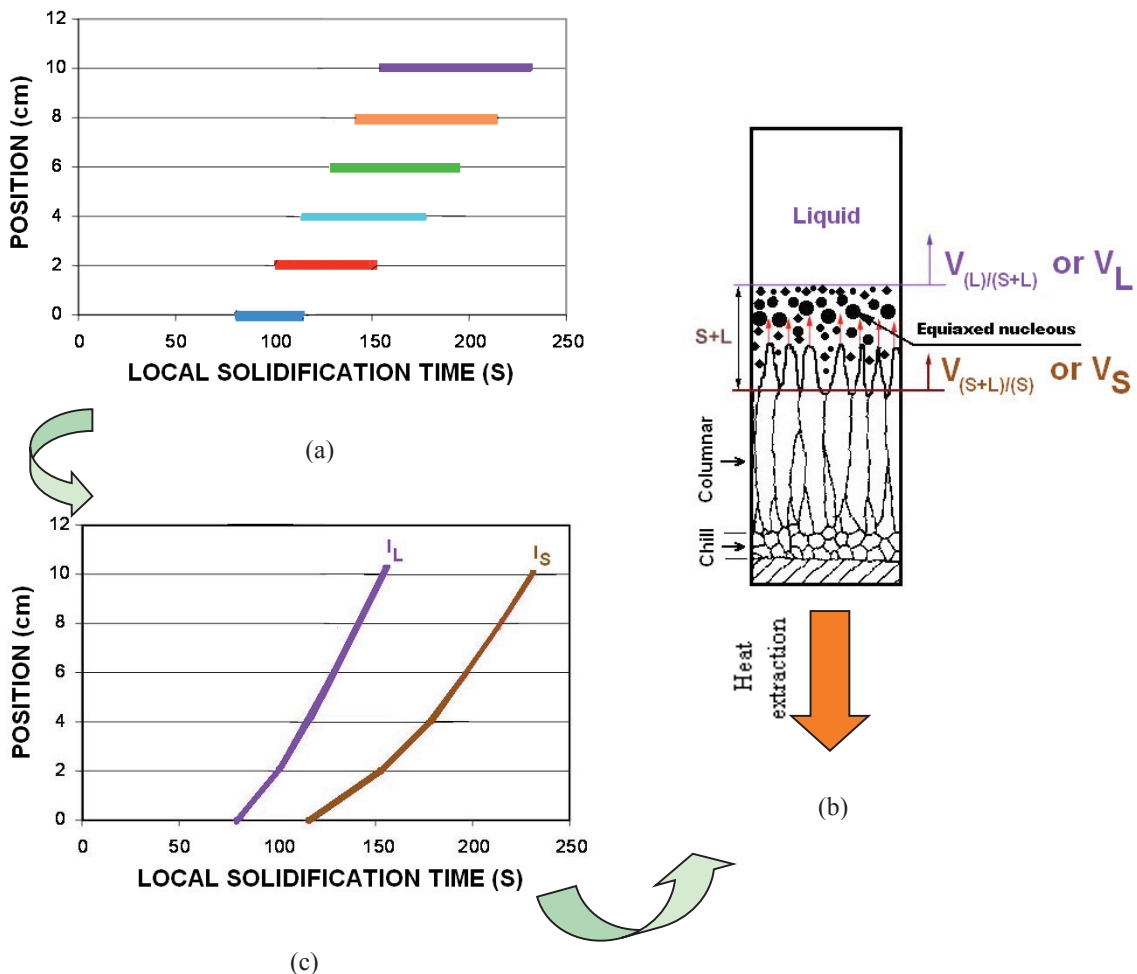


Fig. 6. Interphase position versus time during solidification of composites. (a) ZA27+8vol%  $Al_2O_3$ . (b) Schematic. (c) Liquid interphase position ( $I_L$ ) and solid ( $I_S$ ).

In Figure 7 represents the different velocities,  $V_L$  and  $V_S$  obtained for one of the experiments. In this case both, velocities of the solid and liquid interphase accelerate during, and after the transition, leading to a larger mushy zone.

In Table 2 the highlighted boxes correspond to the liquidus velocities obtained at the critical point of the columnar to equiaxed transition. The observation here is that these values are nearly the largest obtained in each experiment indicating the acceleration of the liquidus interphase at the CET.

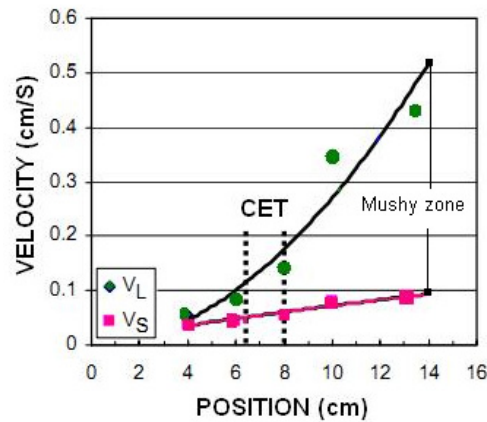


Fig. 7.  $V_L$  and  $V_S$  versus time showing the acceleration of the liquidus interphase from the CET and the increasing in size of the mushy zone.

Table 2. Liquid interface velocity ( $V_L$ ) and solid ( $V_S$ ) and local solidification velocity ( $V_{SL}$ ).

#	Composite	$V_L$ (cm/S)	$V_S$ (cm/S)
1	ZA27+5vol% $Al_2O_3$	0.05	0.02
2	ZA27+5vol% $Al_2O_3$	0.19	0.09
3	ZA27+5vol% $Al_2O_3$	0.22	0.13
4	ZA27+8vol% $Al_2O_3$	0.11	0.05
5	ZA27+8vol% $Al_2O_3$	0.09	0.08
6	ZA27+8vol% $Al_2O_3$	0.15	0.07
7	ZA27+16vol% $Al_2O_3$	0.25	0.10
8	ZA27+16vol% $Al_2O_3$	0.32	0.09
9	ZA27+16vol% $Al_2O_3$	0.45	0.17

### 3.4. Temperature gradients

The temperature gradients,  $G$ , were calculated for each pair of neighbour thermocouples as the temperature difference between the thermocouple readings divided by the separation distance between thermocouples.

The values of gradients are plotted in Figure 8 for one experiment of ZA27+5vol%  $Al_2O_3$  composite. It is observed that from the beginning of solidification, the gradients decrease with the time. The minimum value always corresponds to the position of the columnar-to-equiaxed transition. The gradients showed for the experiment in Figure 8 reach a minimum value of 0.52 °C/cm. Therefore, as it is shown in Table 1, the gradients determined in most experiments are negative. When the negative value of gradient is obtained is an indication of a reversal in the temperatures profiles ahead of the liquid front, which could be associated to the recalescence due to massive



nucleation of equiaxed grains, and previously reported and discussed for different alloys (Ares and Schvezov 2000, Ares et al. 2002, Ares et al. 2005, Ares and Schvezov 2007, Gueijman et al. 2010). The fact that in some cases the position of the thermocouples are not located at the precise position where the transition occurs, may prevent detection of the negative gradients which is believe to occur in all cases.

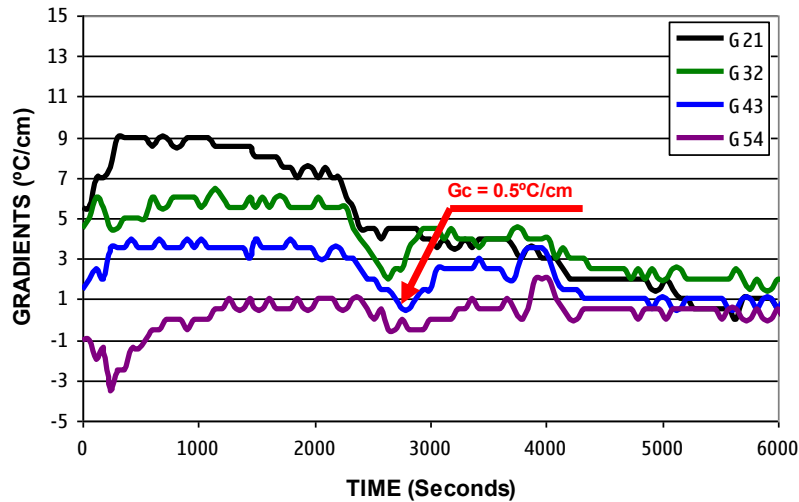


Fig. 8. Temperature gradients versus time. ZA27+5vol% Al<sub>2</sub>O<sub>3</sub>.

#### 4. Conclusions

The main results obtained in the present investigation on directional solidification of Al<sub>2</sub>O<sub>3</sub>-reinforced Zinc-Aluminum matrix composites are summarized as follows:

- Directional solidification of metal matrix composites was performed and the temperatures during the whole process measured in the liquid and solid phases of composites.
- For the three type of composites studied the columnar-to-equiaxed transition was produced and the values of the temperature gradients, which were calculated, reached minimum values during the transition; in most cases even negative.
- As was reported before for ZA alloys, an increase in the cooling velocity in the liquid increases the columnar zone length.
- At the CET, the liquidus interphase velocities are between 0.05 to 0.45 mm/s depending on composite directional solidification experiment.
- Recalescence was detected and measured during the equiaxed transition being of the order of 3.3°C to 1.0°C.
- The transition from columnar-to-equiaxed structure is not abrupt but occurs in a zone of 1 cm or larger and the same results were obtained for the binary Zinc-Aluminum alloys.

#### Acknowledgements

This work was partially supported by the Argentinean Research Council (CONICET) and the National Agency for Science and Technology (PICT-2011-1378).

## References

- Ares, A.E., Schvezov, C.E., Solidification Parameters during the Columnar-to-Equiaxed Transition in Lead-Tin Alloys. *Metallurgical and Materials Transactions*, 31A (2000) p.p. 1611-1625.
- Ares, A.E., Gueijman, S.F., Schvezov, C.E., 2002. Semi-Empirical Modeling for Columnar and Equiaxed Growth of Alloys. *J. Crystal Growth* 241, 235-240.
- Ares, A.E., Gueijman, S.F., Caram, R., Schvezov, C.E., 2005. Semi - Empirical Modeling for Columnar and Equiaxed Growth of Alloys. *J. Cryst. Growth*, 275, 319-325.
- Ares, A. E., Schvezov, C. E., 2007. Influence of Solidification Thermal Parameters on the Columnar-to-Equiaxed Transition of Aluminum-Zinc and Zinc-Aluminum Alloys. *Metall. Mater. Trans. A* 38, 1485-1499.
- Ares, A. E., Schvezov, C. E., 2010. Experimental Study of the Columnar-to-Equiaxed Transition during Directional Solidification of Zinc-Aluminum Alloys and Composites. *World Journal of Engineering*.
- Ares, A.E., Schvezov, C.E., 2013. Columnar-to-Equiaxed Transition in Metal-Matrix Composites Reinforced with Silicon Carbide Particles. *Journal of Metallurgy*. In Press.
- Auras, R., Schvezov, C.E., 2004. Wear Behavior, Microstructure, and Dimensional Stability of As-Cast Zinc-Aluminum / SiC (Metal Matrix Composites) Alloys. *Metallurgical and Materials Transactions A* 35, 1579-1590.
- Gandin, Ch.-A., 2000. Experimental Study of the Transition from Constrained to Unconstrained Growth During Directional Solidification. *ISIJ International* 40, 971-979.
- Gandin, Ch. A., 2000. From Constrained to Unconstrained Growth During Directional Solidification. *Acta Materialia* 48, 2483-2501.
- Gueijman, S. F., Schvezov, C. E., Ares, A. E., 2010. Directional Solidification and Characterization of Zn-Al and Zn-Ag Diluted Alloys. *Materials Transactions* 51, 1851-1870.
- Hunt, J.D., 1984. Steady State Columnar and Equiaxed Growth of Dendrites and Eutectic. *Mater. Sci. Eng.* 65, 75-83.
- Karni, N., Barkay, G.B., Bamberger, M., 1994. Structure and Properties of Metal-Matrix Composites. *Journal of Materials Science Letters* 13, 541-544.
- Mahapatra, R.B., Weinberg, F., 1987. The Columnar to Equiaxed Transition in Tin-Lead Alloys. *Metall. Trans. B* 18, 425-432.
- McFadden S., Browne D.J., Gandin Ch.-A., 2009. A Comparison of CET Prediction Methods using Simulation of the Growing Columnar Front. *Met. Mat. Trans.* 40A, 662-672.
- Moffatt, W.J. 1984. *Handbook of Binary Phase Diagrams*, Published by General Electric Company Corporate Research and Development Technology Marketing Operation, New York, p.p. 259, 419, 437, 391.
- Reinhart, G., Manginck-Noël, N., Nguyen-Thi, H., Schenk, T., Gastaldi, J., Billia, B., Pino, P., Härtwig, J., Baruchel, J., 2005. Investigation of columnar-equiaxed transition and equiaxed growth of Aluminium based alloys by x-ray radiography. *Materials Science and Engineering A* 384, 413-414.
- Speyer, R. F., 1994. *Thermal Analysis of Materials*, Dekker, M. (Ed.), New York, p.p. 30-109.
- Spittle, J.E., 2006. Columnar-to-Equiaxed Grain Transition in as Solidified Alloys, *International Materials Reviews* 51, 247-269.
- Underwood, E.E., 1968. In *Quantitative Microscopy*. De Hoff, R.T. and Rhines, F.N. (Eds.), Mc Graw-Hill Book Co., New York, NY, p.p. 76-101, and p.p. 149-99.
- Vander Voort, G.F., 2000. In: *Metallography Principles and Practice*, ASM International, New York, p.p. 528-761.
- Yasuda, H., Ohnaka, I., Sugiyama, A., Nagira, T., Tsukihara, N., Kawasaki, K., Umetani, K., 2006. Modeling of Casting, Welding and Advanced Solidification Processes – XI<sup>th</sup>. In: Gandin, Ch. A. and Bellet, M., (Ed.). TMS (The Minerals, Metals & Materials Society), Warrendale, P.A., p.p. 375-382.
- Zhu, Y.T., Devletian, J.H., 1994. Application of Differential Thermal Analysis in Phase Diagram Determination. *Journal of Phase Equilibria*, 15, 37-41.
- Ziv, I., Weinberg, F., 1989. The Columnar-to-Equiaxed Transition in Al 3 Pct Cu. *Metallurgical and Materials Transactions A* 20, 731-734.